TÜBİTAK

Turkish Journal of Earth Sciences

http://journals.tubitak.gov.tr/earth/

Research Article

Turkish J Earth Sci
(2019) 28: 438-456

doi:10.3906/yer-1811-7

Mineralogy and geochemistry of feed coals and combustion residues of the Kangal power plant (Sivas, Turkey)

Ali İhsan KARAYİĞİT[1,*], **Rıza Görkem OSKAY**[1], **Rod A. GAYER**[2]

[1]Department of Geological Engineering, Faculty of Engineering, Hacettepe University, Ankara, Turkey
[2]Department of Earth Sciences, Cardiff University, Cardiff, United Kingdom

Received: 13.11.2018 • **Accepted/Published Online:** 03.04.2019 • **Final Version:** 10.05.2019

Abstract: This study focuses on mineralogical and geochemical compositions of feed coal (FC) and combustion residues, namely fly ash (FA) and bottom ash (BA) samples, obtained from the Kangal coal-fired power plant in central Turkey. The X-ray powder diffraction data indicate that carbonate and clay minerals are dominant phases in the FC samples. In the FA samples, quartz, hematite, anhydrite, lime, and feldspar are generally dominant and abundant phases, whereas calcite, ettringite, and portlandite are generally more abundant in the BA samples. The elements Mo, Cs, and U are significantly enriched in the studied FC, FA, and BA samples. The statistical analysis and SEM-EDX data show that Ca, Ti, and the vast majority of trace elements are inorganically affiliated, and only Tl and U have probable organic affinity in the FC. In addition, the redox conditions in the paleomires presumably resulting in Mo and U enrichment in FC, whereas their enrichment in FA and BA is most likely related to retention by CaO and Ca-sulfate. The Cs enrichment in FA is due to retention by glass. The elements in the FA and BA are distinguished into four groups according to their volatility during combustion. The elements As, Mo, Cd, Tl, and U (Group I) are the most volatile elements during combustion and condensation in the FA. The elements Li, Zn, Ga, Rb, Nb, Cs, Ba, La, and Pb (Group IV) did not become more volatile or less volatile during combustion and are located in BA. Nevertheless, Zn and Pb in the BA seem to be related to the presence of unaffected pyrite and sphalerite, and are due to low combustion efficiency of the boiler during the sampling period. Overall, enriched elements and minerals in FA and BA suggest that their disposal should be undertaken with caution.

Key words: Kangal, coal, fly ash, combustion, elemental enrichment, mineralogy, geochemistry

1. Introduction

Coal is a primary local energy resource in Turkey, and the country's energy demand has increased remarkably during the last decade. As a result, several coal-fired power plants are under construction. The total coal reserves of Turkey reach around 17 Gt and are mostly composed of Cenozoic, low-rank coals, which display high ash yields and total sulfur contents (Karayigit et al., 2000; Tuncalı et al., 2002; Oskay et al., 2013). Furthermore, environmentally sensitive elements (e.g., B, Cr, As, and Ni) are enriched in these coals (Querol et al., 1997; Karayigit et al., 2000; Palmer et al., 2004) and consequently have potential adverse effects on environment and human health. Their total geological reserves and low calorific values make these coals suitable for energy generation. Considering their high ash yields, total sulfur contents, and elemental enrichment, emission of hazardous trace elements and disposal of combustion residues of the power plant will be problematic in the near future for the Turkish energy sector. Therefore, the determination of the mineralogical and geochemical features of feed coals (FCs) and combustion residues is essential. Recently, some environmental problems related to disposal of combustion residues and their potential usage in the cement and brick industry have been reported (e.g., Erol et al., 2000; Baba et al., 2003; Yılmaz, 2012; Akar et al., 2013). Furthermore, some studies have been conducted to understand the mineral and chemical composition of fly ash (FA) and bottom ash (BA) and the partitioning of elements during combustion in Turkish coal-fired power plants (Bayat, 1998; Karayigit et al., 2001a, 2005, 2006; Vassilev et al., 2005a, 2005b; Esenlik et al., 2006; Fotopoulou et al., 2010).

The Kangal coal deposit is located in eastern Central Anatolia and two mineable coal seams (upper and lower) are located within basinal infillings (Figure 1) (Karayigit et al., 2001b; Narin and Kavusan, 1993). The coals are exploited in an open-cast mine (Kalburçayırı) to support the Kangal power plant, which is one of the most important

* Correspondence: aik@hacettepe.edu.tr

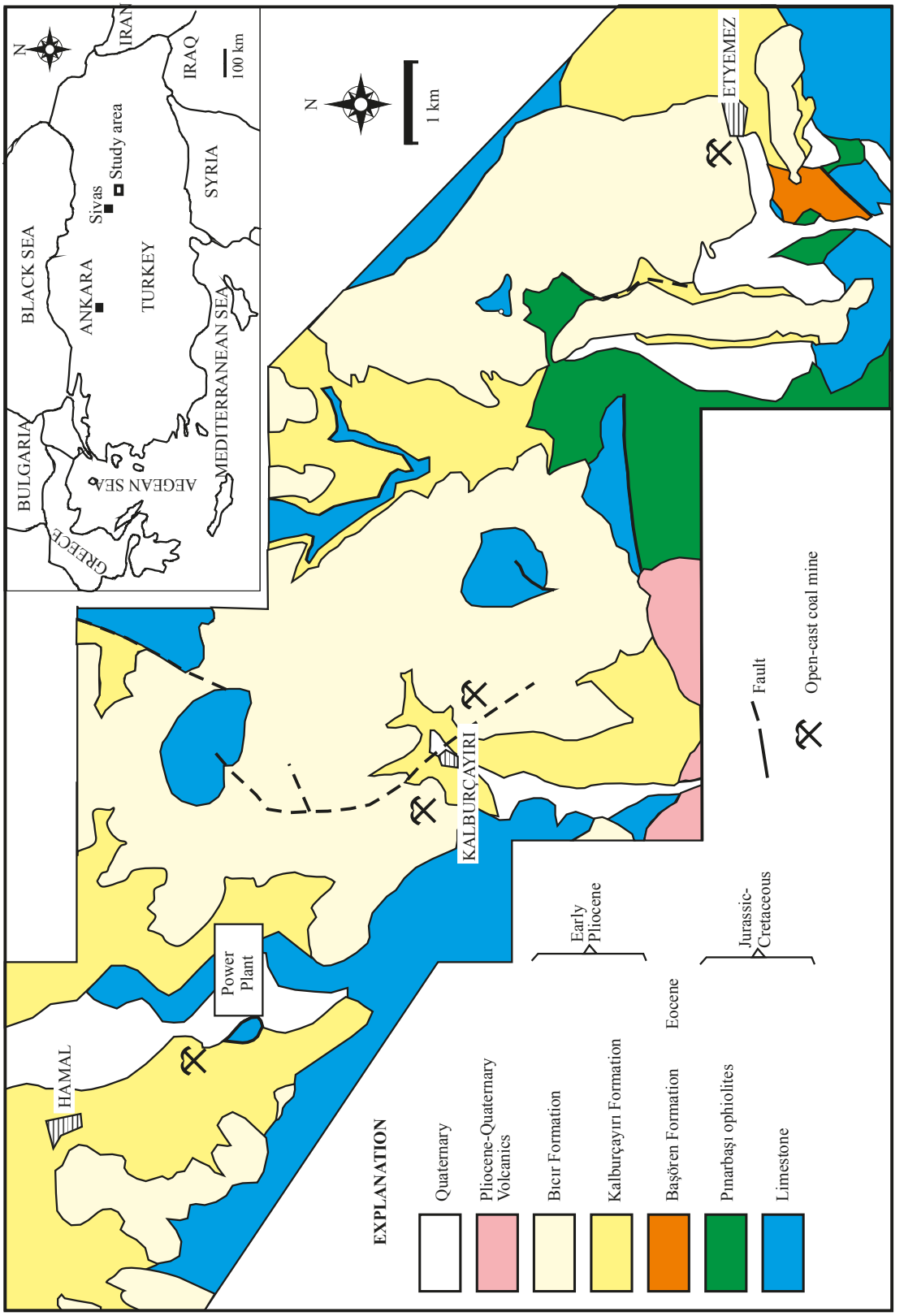

Figure 1. Location and geological map of Kangal coal deposit (modified from Karayiğit et al. (2001b) and Narin and Kavuşan (1993)).

power plants in eastern Turkey and has a 457 MW (2 × 150 and 1 × 157 MW) total installed capacity (Figure 2). The annual coal consumption is around 7 Mt, consumed by three units[1]. The Kangal coal deposit was the subject of several petrographic, geological, and mining utilization studies (Narin and Kavuşan, 1993; Basarir and Karpuz, 2004; Toprak and Yalcin Erik, 2011; Yalçin Erik, 2011; Koçaslan et al., 2017); however, a limited number of studies were focused on geochemical compositions of feed coals and radionuclides of feed coals and combustion residues (Karayigit et al., 2000, 2001b; Kalender and Karamazı, 2017; Turhan et al., 2018). The current study focuses on the mineralogical and geochemical characteristics of FCs and combustion residues (FA and BA) from Unit-I and evaluates factors that control elemental enrichment of FC, FA, and BA.

2. Geological setting

The Kangal coal deposit is located in the southern part of the NE–SW-oriented Sivas Basin (Narin and Kavusan, 1993; Toprak and Yalcin Erik, 2011). The pre-Neogene basement rocks are mainly Jurassic-Cretaceous marine carbonates, ophiolitic rocks (Pınarbaşı ophiolites), and small Eocene marine carbonates outcrops (Narin and Kavusan, 1993; Karayiğit et al., 2001b; Yağmurlu et al., 2016). The Pliocene basinal infillings commence with fluvio-alluvial deposits (Kalburçayırı Formation: conglomerate, sandstone, and claystone). This sequence is followed by lacustrine sediments, which host two mineable coal seams (upper and lower seams). The coal-bearing sequence is composed of alternating siltstone, claystone, coal, and marl. The total thickness of both coal seams is variable and in the Kalburçayırı coalfield reaches 11 m (Karayiğit et al., 2001b). The upper seam contains several partings (≥30 cm), whereas the lower seam includes very thin partings (<10 cm) (Figure 3). These partings are mainly composed of gastropod-bearing calcareous units and tuffaceous/altered tuff layers. The gathered gastropod and ostracod fauna and palynoflora from lower and upper coal seams show that in the Kangal paleomire freshwater conditions dominated during the Early Pliocene (Narin and Kavusan, 1993; Karayiğit et al., 2001b; Yalçin Erik, 2011). The coal-bearing sequence is overlain by Early Pliocene lacustrine carbonates (Bıcır Formation) and Plio-Quaternary volcanics. Finally, Quaternary unconsolidated sediments unconformably overlay all units (Figure 1).

3. Materials and methods

Twenty-five samples each of feed coal, fly ash, and bottom ash, weighing about 5 to 10 kg each, were systematically collected from Unit-I of the Kangal power plant once a week over a 6-month period. In order to avoid combustion temperature and equipment differences among units of the Kangal power plant, the studied FC, FA, and BA samples were only taken from the pulverized coal fired boiler in Unit-I. In total 75 samples (25 FCs, 25 FAs, and 25 BAs) were obtained and examined in this study. The FC samples were mined from the Kalburçayırı coalfield and sampled from the boiler mills. The FA samples were collected from electrostatic precipitation sampling (ESP) points and split for analysis, whereas the BA samples were obtained from the boiler doors under the boiler. No pulverized rejects were included in the BA samples.

The proximate, total sulfur, and gross calorific value analyses of the studied FC samples were carried out at Hacettepe University according to standard procedures (American Society for Testing and Materials, 2003, 2008, 2011, 2017).

The mineralogical compositions of the studied FC, FA, and BA samples were determined using X-ray powder diffraction (XRD) with a Cu anode tube at Cardiff University. The scanning area covered the 2θ interval between 3° and 70°, with a scanning angle step of 0.015° and a step time of 1 s. The elemental compositions of coal samples were determined using inductively coupled plasma-mass spectrometry (ICP-MS) at Cardiff University. Samples for ICP-MS were prepared following the method described by Gayer et al. (1999). Two hundred milligrams of coal and combustion residues were sequentially digested, using concentrated HF, aqua regia, and 5 M HCl. Samples were then volumetrically diluted to 3 to 100 mL in deionized water. Sample solution (5 mL) was then analyzed for a wide range of trace elements. The SARM 18, 19, and 20 standards also were digested to determine the accuracy of the method. Furthermore, polished blocks were prepared from selected FC, FA, and BA samples. These blocks were coated with carbon and were investigated under a Zeiss EVO-50 EP SEM-EDX at Hacettepe University to better understand the mineralogical and geochemical compositions of FC, FA, and BA samples.

Figure 2. General view of Kangal power plant.

[1]http://kangaltermik.com.tr/Tr/kurumsal

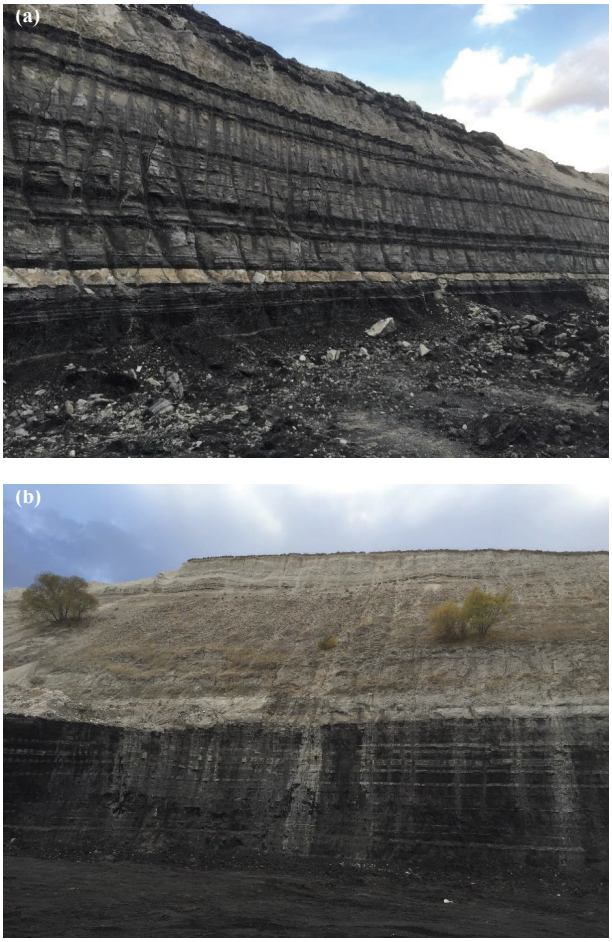

Figure 3. General view of (a) the upper seam and (b) the lower seam in the Kalburçayırı open-cast mine.

4. Results

4.1. Feed coal samples

4.1.1. Standard coal characteristics

Macroscopically, the studied FC samples are black in color and mostly contain bands bearing fossil shell remains. These bands are characteristic for coal seams in the Kangal coalfield (Karayiğit et al., 2001b; Toprak and Yalcin Erik, 2011). The studied FC samples display high total moisture (43.1%–55.8%, avg. 47.9%, as-received basis), volatile matter contents (37.7%–46.2%, avg. 40.2% on dry basis), and total sulfur contents (3.2%–5.6%, avg. 3.9% on dry basis). The ash yields of the FC samples are high and range widely (31.8%–64.0%, avg. 54.5 on dry basis). In turn, gross calorific values are slightly low and variable (Table 1). The high ash yields and volatile matter contents are related to be the presence of fossil-bearing zones in both of the coal seams. The breakdown of these remains could elevate particularly volatile matter contents and ash yields. A similar assumption was also proposed for high volatile matter and ash yields of coal samples in the Kalburçayırı coalfield (Karayiğit et al., 2001b). Overall, the standard coal features of the studied FCs are consistent with previous studies from borehole and open-cast mines in the Kangal coal deposit (Narin and Kavusan, 1993; Karayiğit et al., 2001b; Tercan and Karayiğit, 2001; Toprak and Yalcin Erik, 2011).

4.1.2. Mineralogical composition

The minerals identified applying X-ray diffraction in the studied bulk FC samples are mainly composed of calcite, clay minerals (illite and kaolinite), quartz, pyrite, aragonite, and feldspars (Table 2). Furthermore, opal/CT gypsum and apatite were identified in some FC samples. Similar mineralogical compositions were also identified from open-cast mines in the Kangal coal samples from both the deposit and the power plant (Karayiğit et al., 2000, 2001a). The results of SEM-EDX studies of FC samples are in agreement with XRD results, and several accessory minerals such as barite, cassiterite, celsian, galena, ilmenite, manganite, native silver, rhodochrosite, sphalerite, sphene, Ti-oxides, zircon, and unidentified ferromagnesian silicate mineral were identified (Figure 4). In addition, calcareous fossil shell remains, diatomite, and silica glass shards were also identified by SEM-EDX analyses in some FC samples.

Calcite is the dominant phase in all studied FC samples while aragonite is, in general, a minor phase. The dominance of carbonate minerals in the studied FC samples is related to bands bearing fossil shell remains; this also indicates Ca-rich water influence on the paleomire (Figures 4a and

Table 1. Ranges and averages (in parentheses) of the values obtained from proximate and ultimate analyses of feed coal, fly ash, and bottom ash samples (ar: as-received basis, wt.%: weight, %, GCV: gross calorific value).

Analyses	Feed coal	Fly ash	Bottom ash
Total moisture (wt.%, ar)	43.1–55.8 (47.9)	-	-
Volatile matter (wt.%, dry)	37.7–46.2 (40.2)	-	-
Ash (wt.%, dry)	31.8–64.0 (54.5)	93.1–98.7 (97.5)	62.9–91.3 (77.6)
Total S (wt.%, dry)	3.2–5.6 (3.9)	2.8–5.3 (3.8)	0.9–2.7 (1.7)
GCV (MJ/kg, dry)	8.7–15.8 (11.7)	-	-

Table 2. Mineralogical compositions of feed coal, fly ash and bottom ash samples from the Kangal power plant based on XRD and SEM-EDX studies (+++ = dominant phase, ++ = abundant phase, + = minor phase, ± = detected in a few samples through XRD, a: accessory mineral detected through SEM analysis).

Mineral	Feed coal	Fly ash	Bottom ash
Quartz	++	+++	++
Cristobalite	±	+	+
Clay minerals	+++		a
Feldspars	+	++	+
Melilite group		+	+
Sphene	a		
Zircon	a		a
Pyrite	++	a	a
Pyrrhotite		a	a
Sphalerite	a		a
Galena	a		
Gypsum	±		
Anhydrite		++	+
Ettringite		+	+
Barite	a	a	a
Calcite	+++	+	+++
Aragonite	+		
Rhodochrosite	a		
Apatite	±	a	a
Monazite	a	a	a
Hematite		+++	++
Spinel		+	+
Portlandite		+	+++
Cassiterite	a		
Ilmenite	a	a	a
Lime		++	++
Ti-oxides	a	a	a

4b) (Querol et al., 1996; Karayiğit et al., 2017b). The SEM study proved that the clay minerals appear as aggregates with other minerals (e.g., quartz, feldspars, apatite, Ti-oxides, monazite, and zircon) and organic matter (Figures 4c and 4d). Such associations generally imply clastic input from basement rocks outcropping in the basinal margins (Karayiğit et al., 2001b, 2017a; Siavalas et al., 2009). Considering the presence of tuff layers within coal seams and silica glass shards in the studied FC samples, aluminosilicates, accessory phosphates, and zircon in the studied FC samples could also have originated from reworked tuff and/or synchronous volcanic input into the Kangal paleomire (Bohor and Triplehorn, 1993; Burger et al., 2000). The presence of kaolinite originating from altered volcanic input in the FC samples might be related to open system and/or low pH conditions in the paleomire, where volcanic glass shards are unstably altered to clay minerals (Dai et al., 2017). Nevertheless, its coexistence with apatite in the FC samples points to a low weathering degree of volcanic input under neutral conditions (Bohor and Triplehorn, 1993). Thus, weak acidic to neutral conditions might have dominated in the Kangal paleomire.

Framboidal pyrite is the most common mineral in the FC samples, while euhedral pyrite and pyrite infillings within cavities of calcareous fossil remains were identified in some samples (Figures 4e–4h). These crystallization morphologies generally reflect a syngenetic origin for pyrite, which also implies a sulfate-rich ground water supply from Cretaceous carbonates in the basement into the paleomire (Oskay et al., 2016; Ward, 2016). Their coexistence with calcareous fossil remains and diatomite could suggest the development of weak acidic to neutral conditions in the Kangal paleomire. Galena is generally associated with clay minerals, and individual sphalerite was rarely identified. Thus, galena might be epigenetically precipitated from intraseam solutions and/or leached solutions from tuff layers within the deposit (Dai et al., 2015; Karayiğit et al., 2017a, 2018). The individual sphalerite, along with cassiterite and native silver, could be clastic input from alteration zones in the basement rocks and/or epigenetic precipitation from circulated solutions within the coal seams (Marschik et al., 2008; Kuşcu et al., 2013; Dai et al., 2015; Karayiğit et al., 2018). Barite is associated with framboidal pyrite clusters in some FC samples (Figures 4f and 4g). These associations imply a possible syngenetic origin for barite (Rudmin et al., 2018). Furthermore, barite is also observed as cleat/fracture infillings that indicate an epigenetic origin for barite (Figure 4h). In low-rank coals, gypsum could easily form via pore water evaporation during transport and storage, along with oxidation of pyrite in the stockpiles (Koukouzas et al., 2010; Oskay et al., 2016; Ward, 2016). Both cases are possibly developed in the studied FC samples; thus, gypsum in the studied samples has epigenetic origin.

4.1.3. Geochemistry

The ICP-MS results show that Ca, Mg, and Ti are major elements (≥1000 μg/g) in the studied FC samples (Table 3). The elements that have average concentrations exceeding 100 μg/g are P, Mn, Sr, Mo, Ba, and Zn, while average concentrations of rare earth elements and Y (REY) are generally less than 1 μg/g (Table 3). The ranges of values for elements in the studied FC samples are variable.

4.2. Fly and bottom ash samples

4.2.1. Proximate analyses data

The ash yields of BA samples, as expected, are lower than those of FA samples due to the presence of unburned

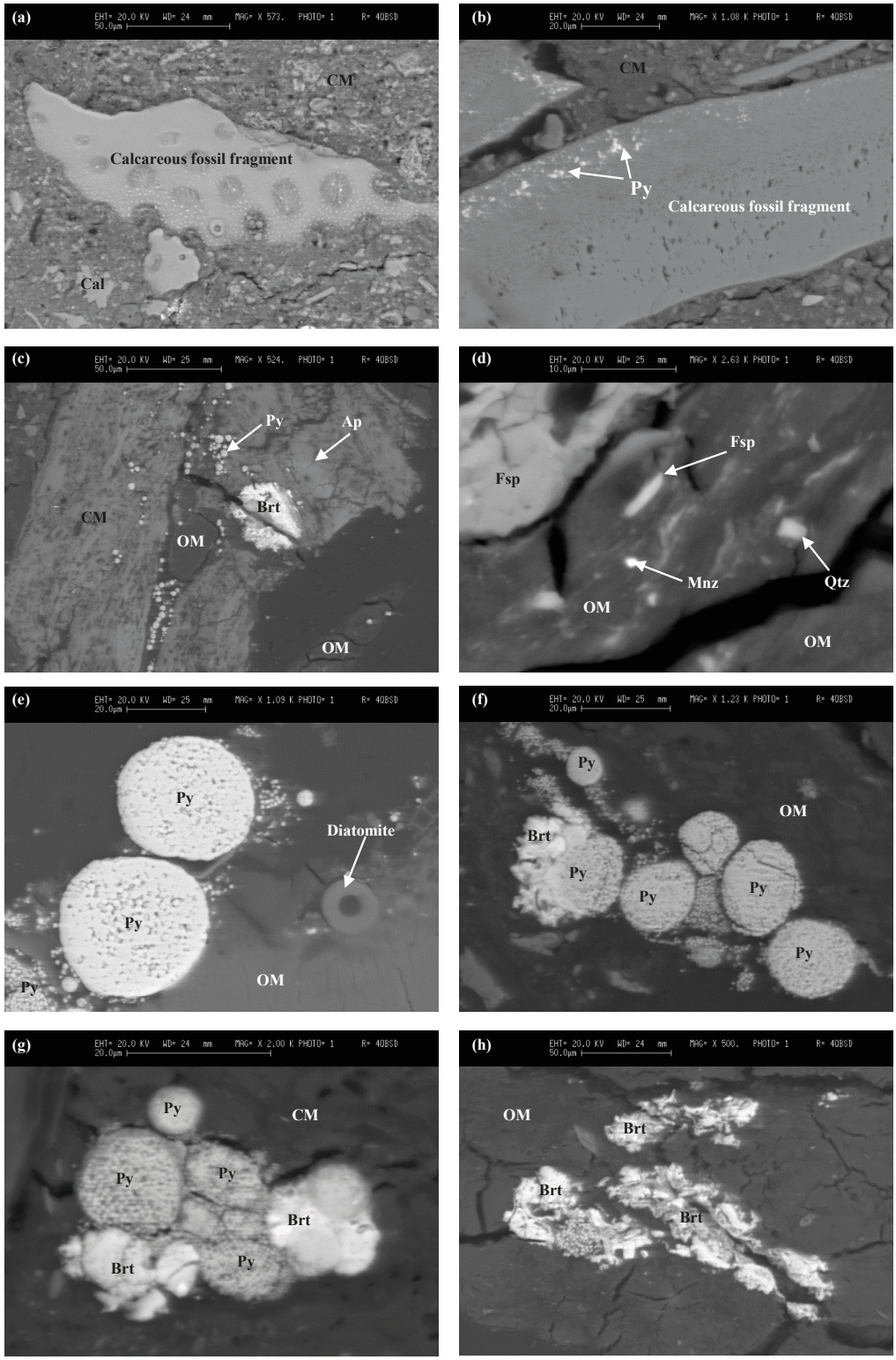

Figure 4. Scanning electron backscattered images of crystalline phases in the feed coal of Kangal power plant: (a and b) clay minerals (CM) associated with calcite (Cal), calcareous fossil shell fragments and pyrite (Py); (c) clay minerals (CM) associated with organic matter (OM), apatite (Ap), barite (Brt), and pyrite (Py); (d) organic matter (OM) associated with feldspar (Fsp), quartz (Qtz), and monazite (Mnz); (e) organic matter (OM) associated with pyrite (Py) and diatom remains; (f and g) pyrite crystals (Py) associated with barite (Brt) and organic matter (OM)/clay minerals (CM); (h) cleat/fracture infillings barite (Brt).

Table 3. The ranges and averages of the elements (in μg/g, unless otherwise indicated) in the studied FC samples, and their comparison with worldwide coals (a: from Swaine (1990) and b: from Ketris and Yudovich (2009)).

Elements	Kangal FC		Most world coals[a]	World low-rank coals[b]
	Range	Average		
Ca, %	4.7–14.2	9.6	-	-
Mg, %	0.5–0.9	0.7	-	-
Li	25–40	32	1–80	10
Be	0.67–1.4	0.91	0.1–15	1.2
P	443–696	542	10–3000	200
Sc	4.2–7.4	5.6	1–10	4.1
Ti, %	0.12–0.19	0.15	0.001–0.2	0.72
Cr	50–89	71	0.5–60	15
Mn	58–195	140	5–300	100
Co	4.6–12	6.7	0.5–30	4.2
Cu	7.9–20	18	0.5–50	15
Zn	41–178	129	5–300	18
Ga	5.0–8.3	6.8	1–20	5.5
Ge	0.13–1.0	0.70	1–50	2
As	62–90	71	0.5–80	7.6
Rb	17–50	31	2–50	10
Sr	422–807	606	15–500	120
Y	5.3–11	7.8	2–50	8.6
Zr	31–49	42	5–200	35
Nb	4.4–9.8	6.2	3–30	11
Mo	80–127	101	0.1–10	2.2
Cd	0.21–0.71	0.38	0.1–3	0.24
Sb	1.4–3.4	2.8	0.5–10	0.84
Cs	13–25	20	0.1–5	0.98
Ba	56–588	205	20–1000	150
La	6.6–13	11	1–40	10
Ce	13–25	20	2–70	22
Pr	1.5–2.8	2.3	1–10	3.5
Nd	5.5–10.6	8.4	3–30	11
Sm	1.1–2.0	1.6	1–6	1.9
Eu	0.29–0.59	0.46	0.1–2	0.5
Gd	1.0–2.2	1.7	0.1–4	2.6
Tb	0.16–0.33	0.25	0.1–1	0.32
Dy	0.9–1.8	1.4	1–4	2
Ho	0.17–0.38	0.27	0.1–2	0.5
Er	0.5–1.1	0.8	1–3	0.85
Tm	0.08–0.16	0.11	0.5–3	0.31
Yb	0.50–0.99	0.74	0.3–3	1
Lu	0.07–0.15	0.11	0.03–1	0.19
Hf	1.0–1.6	1.3	0.4–5	1.2
Ta	0.41–1.5	0.66	0.1–2	0.26
W	0.87–3.6	1.7	0.5–5	1.2
Tl	3.6–6.2	4.9	0.2–1	0.68
Pb	6.3–64	20	2–80	6.6
Bi	0.11–0.37	0.18	2–20	0.84
Th	2.6–5.2	3.9	0.5–10	3.3
U	27–44	37	0.5–10	2.9

coal particles in BA samples (Table 1). These particles also caused measurable calorific values from BA samples. The average total S content of the FA samples is almost threefold higher than that of the BA samples (Table 1). During combustion in boilers, sulfur in FCs becomes volatile and is mostly captured by FA particles in the boiler and/or emitted into the atmosphere. Therefore, total S content of FA is generally higher than in BAs (Karayigit et al., 2001a; Vassilev et al., 2005a; Esenlik et al., 2006). This process also explains the relatively higher total S content of the studied FA samples. Even though the petrographic features of studied FA and BA samples were not examined in detail, inorganic fractions (mineroids and nonmineroids, as classified in the ICCP nomenclature) are commonly observed during SEM studies (Suárez-Ruiz et al., 2017). Glassy materials and Fe-oxides are the most common inorganic fractions in the FA and BA samples, whereas unaffected coal particles were also rarely observed in some FA and BA samples during SEM studies (Figures 5 and 6). The presence of unburned coal particles in the BA could be related to either pulverized rejects or low combustion efficiency of boilers in power plants (Styszko-Grochowiak et al., 2004; Hower et al., 2017). Taking into account the absence of pulverized rejects in the studied BA, the unaffected coal particles could imply occasional low combustion efficiency of the boiler of Unit-I, at least during the sampling period. Similarly, unaffected coal particles were also reported from other pulverized coal fired boilers in Turkey (Karayigit et al., 2001a; Vassilev et al., 2005a; Esenlik et al., 2006).

4.2.2. Mineralogical composition

The mineralogical compositions of the studied FA and BA samples were similar, and the following minerals were identified applying XRD: quartz, feldspars, anhydrite, lime, hematite, calcite, ettringite, cristobalite, hercynite, gehlenite, and portlandite (Table 2). The quartz, hematite, anhydrite, lime, and feldspar are generally the most dominant and abundant phases in the FA samples, whereas calcite, ettringite, and portlandite are generally more abundant in the BA samples (Table 4). The SEM-EDX analyses of FA and BA are also in agreement with the XRD results. Apatite, barite, Fe-oxides, FeCrTi-oxides, ilmenite, monazite, pyrite, pyrrhotite, Ti-oxides, and unidentified FeCaAl- and FeMg-silicate minerals are the accessory minerals in the studied FA samples, whereas in the BA samples apatite, barite, Fe-oxides, kaolinite, ilmenite, monazite, pyrite, pyrrhotite, sphalerite, Ti-oxides, and zircon are identified as accessory minerals (Figures 5a–5h and 6a–6h).

Quartz and feldspars in FCs are generally considered as refractory minerals (Querol et al., 1994; Reifenstein et al., 1999; Vassilev et al., 2005b). Nevertheless, these minerals could also be formed during combustion (Vassilev and Vassileva, 1996; Moreno et al., 2005; Vassilev et al., 2005a).

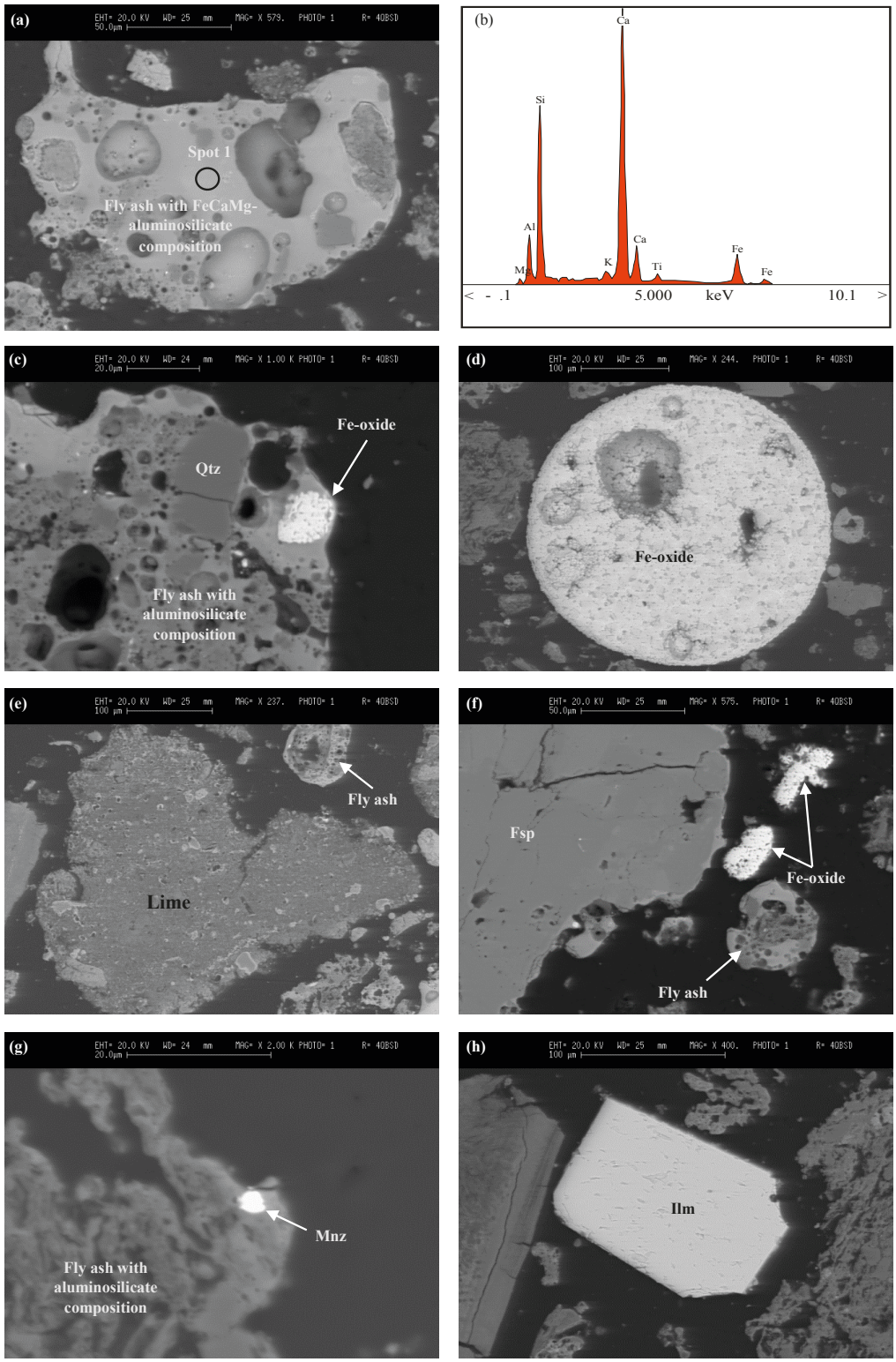

Figure 5. Scanning electron micrograph backscattered images of crystalline phases in the fly ash (FA) of Kangal power plant: (a) FA of mainly Ca, Fe, and Mg alumonisilicate composition; (b) EDX data of FA on spot 1 (see Figure 5a); (c) FA with mainly aluminosilicate composition and Fe-oxides and quartz (Qtz) within pores; (d) FA of Fe-oxide composition; (e) lime and FA of mainly aluminosilicate composition; (f) feldspar (Fsp), FA of aluminosilicate composition, and Fe-oxide; (g) FA aluminosilicate composition and monazite (Mnz) within pore; (h) ilmenite.

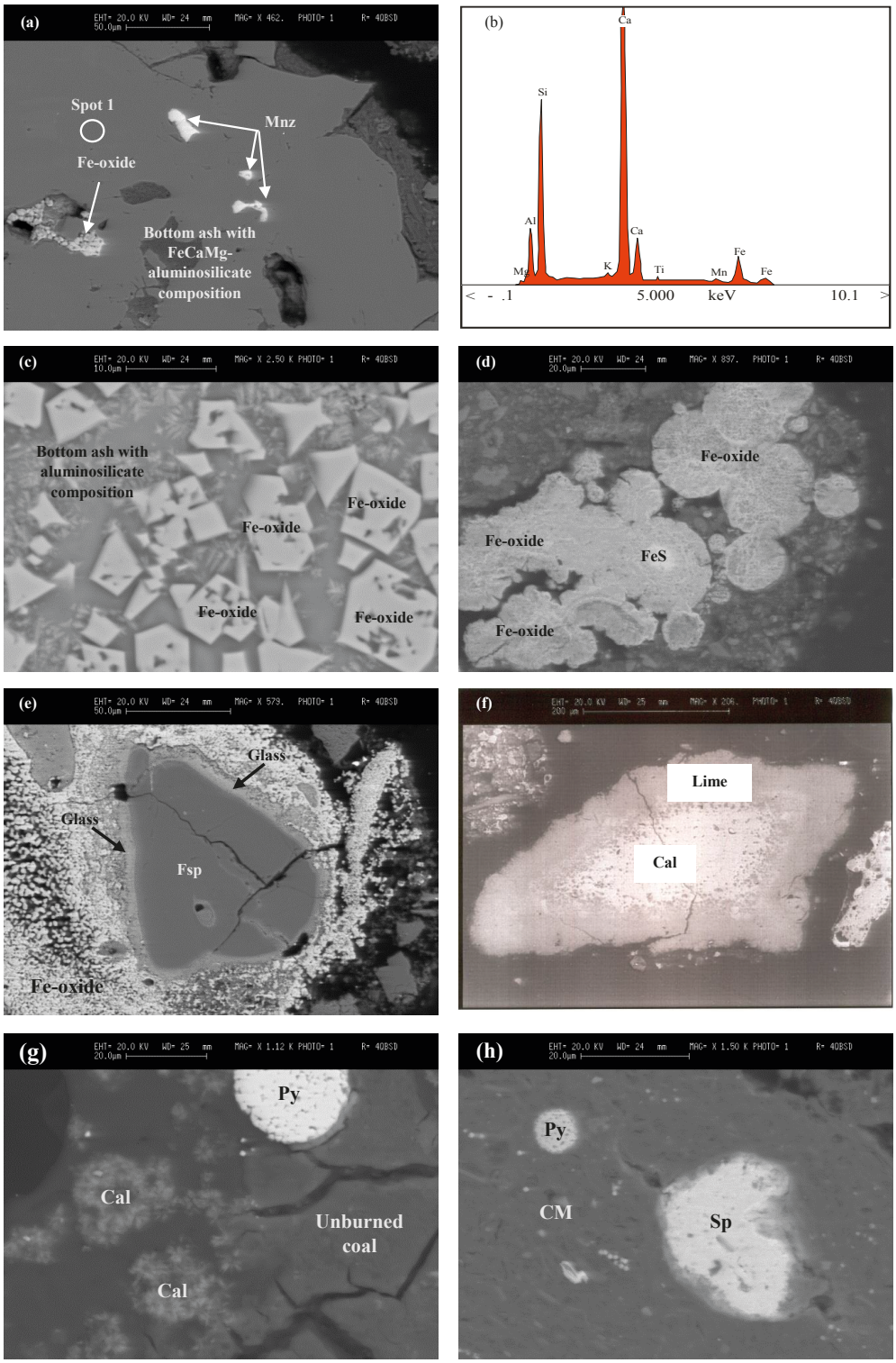

Figure 6. Scanning electron backscattered images of crystalline phases in the bottom ash (BA) of Kangal power plant: (a) BA of mainly Mg, Fe, and Ca alumonisilicate composition; (b) EDX data of FA on spot 1 (see Figure 6a); (c) BA of alumonisilicate composition associated with Fe-oxides; (d) Fe-oxide and FeS association with possible framboidal relics; (e) reacted feldspar (Fsp) and overgrowth glass, and unaffected pyrites (Py); (f) reacted syngenetic carbonate (Cal) and overgrowth lime; (g) unburned coal fragment and primary calcite (Cal) and framboidal pyrite crystals (Py); (h) unaffected clay mineral matrix (CM) associated with pyrite (Py) and Pb-bearing sphalerite (Sp).

Table 4. The ranges and averages of the elements (in μg/g, unless otherwise indicated) in the studied FA and BA samples, and their comparison with worldwide brown coal ashes (a: from Ketris and Yudovich (2009).

Elements	Kangal FA		Kangal BA		World brown coal ashes[a]
	Range	Average	Range	Average	
Ca, %	18.1–26.6	22.3	14.5–26.8	18.7	-
Mg, %	1.3–2.1	1.6	1.2–2.0	1.6	-
Li	64–88	77	74–109	92	49
Be	1.7–2.4	2.1	1.7–3.2	2.5	6.7
P, %	0.1–0.2	0.1	0.08–0.1	0.1	1.2
Sc	11–19	14	9.2–19	15	23
Ti, %	0.3–0.4	0.4	0.3–0.5	0.4	4.0
Cr	137–246	167	112–218	177	82
Mn	267–416	334	269–438	350	550
Co	13–17	15	12–18	15	26
Cu	36–77	45	28–52	40	74
Zn	215–410	282	181–443	317	110
Ga	14–19	16	12–21	18	29
Ge	0.4–2.0	1.2	0.2–2.6	1.0	11
As	84–236	143	53–120	81	48
Rb	65–86	75	73–124	98	48
Sr	1154–1850	1448	773–1233	944	740
Y	15–21	18	12–22	18	44
Zr	87–119	103	72–124	100	190
Nb	13–19	15	14–23	18	18
Mo	158–265	218	74–148	107	15.0
Cd	0.5–1.1	0.7	0.2–0.8	0.5	1.1
Sb	4.5–8.4	5.8	2.9–5.3	4.3	5.0
Cs	42–56	47	36–63	53	5.2
Ba	238–1633	717	638–1283	863	900
La	23–29	25	20–33	28	32
Ce	43–54	48	36–61	51	59
Pr	4.9–6.4	5.5	4.1–7.2	5.8	6.8
Nd	17–23	20	15–26	21	27
Sm	3.3–4.5	3.9	2.7–5.1	3.9	4.0
Eu	0.9–1.4	1.1	0.9–1.6	1.2	1.0
Gd	3.4–4.6	3.9	2.9–5.1	4.1	16.0
Tb	0.5–0.7	0.6	0.4–0.8	0.6	2.0
Dy	2.9–3.9	3.3	2.4–4.1	3.3	12.0
Ho	0.5–0.7	0.6	0.4–0.8	0.6	3.1
Er	1.5–2.2	1.8	1.2–2.3	1.8	4.6
Tm	0.2–0.3	0.3	0.2–0.3	0.3	1.8
Yb	1.5–2.0	1.7	1.1–2.1	1.7	5.5
Lu	0.2–0.3	0.3	0.2–0.3	0.3	1.1
Hf	2.5–5.0	3.1	2.2–4.0	3.0	7.5
Ta	1.0–3.9	1.6	1.3–3.7	1.7	1.4
W	2.3–5.0	3.7	1.9–11.3	5.2	6.0
Tl	5.9–10.9	8.8	3.5–9.9	6.2	5.1
Pb	18–77	48	16–133	61	38
Bi	0.1–1.0	0.4	0.1–0.3	0.2	4.3
Th	8.3–10	9.2	7.1–11	9.5	19
U	62–106	82	36–77	50	16

Cristobalite (opal-CT) is a minor phase in the FC samples and its presence in the FA and BA samples could suggest that it is also a refractory mineral during combustion. Nevertheless, cristobalite is a generally abundant phase in FA and BA samples (Table 4). This difference might also imply that primary quartz changed to cristobalite during combustion in the boilers. Another source for quartz in the studied combustion residues could be liberated Si from the breakdown of clay minerals (e.g., kaolinite) during combustion (Moreno et al., 2005; Vassilev et al., 2005b).

In some FA and BA samples, unaffected clay minerals were detected as accessory minerals during SEM-EDX studies (Figure 6h); nevertheless, clay minerals generally melt during combustion. The liberated Na, K, Ca, and Fe from decomposition of mineral matter during combustion could easily react with aluminosilicate glass and amorphous silicate and form secondary silicate minerals (e.g., mullite and spinel group minerals) or spheres in the combustion residues (Sokol et al., 2002; Ward and French, 2006; Creelman et al., 2013; Dai et al., 2014). The secondary spinel group minerals (e.g., hercynite) in crystalline phases and unidentified FeCaAl- and FeMg-silicate minerals in the studied FA and BA samples are evidence for these reactions in the sampled boilers. Furthermore, glasses in the FA and BA samples are FeCaAl-silicates in composition based on SEM-EDX results, and K, Ti, Mg, and Mn were also traced from glass (Figures 5a, 5b, 6a, and 6b). Thus, glass in the studied combustion residues seems to be derived from the destruction of clay minerals in the FC during combustion. The SEM-EDX data also show that feldspars reacted during combustion, and glass developed as overgrowths on some feldspars (Figure 6e). Therefore, glass seems to be partly derived from feldspar in the FC samples. The reacted feldspars could also suggest that feldspars in the studied combustion residues decomposed during combustion; hence, feldspars may have derived through reactions between Ca, K, and Na and aluminosilicate glass (Querol et al., 1994; Vassilev et al., 2003; Silva et al., 2014). In addition, the FeCa-rich composition of glass could indicate that liberated Fe and Ca from decomposition of nonsilicate minerals during combustion could take place in the formation of glass in the studied FA and BA samples (Sokol et al., 2002; Dai et al., 2014; Valentim et al., 2016).

Pyrites in the FC were decomposed during combustion and converted to Fe-oxides and pyrrhotite or other FeS phases (Huffman et al., 1989; McLennan et al., 2000). If these phases do not come in contact with aluminosilicate glass, Fe-rich glass could form during combustion (Sokol et al., 2002; Valentim et al., 2016). In the studied samples, both Fe-oxides and Fe-rich glass were identified in combustion residues through the SEM-EDX examination (Figures 5a–5d and 6a–6d); hematite is abundant in FA and BA samples (Table 2). Additionally, pyrrhotite, Fe-oxide-

pyrite associations, and unaffected pyrites were identified from both FA and BA samples. These assemblages could relate to either the low-efficiency of the boiler or the reduced atmospheric conditions in the sampled boilers (Spliethoff et al., 1996; Bryant et al., 1999; McLennan et al., 2000).

Carbonate minerals are the dominant phases in the FC samples, and their breakdown during combustion resulted in the formation of lime (CaO) in the boiler (Filippidis et al., 1996; Vassilev and Vassileva, 1996; Fernandez-Turiel et al., 2004). The CaO generally reacts with SO_x in the boiler atmosphere, resulting in the formation of sulfate minerals in the FA and BA (Huffman et al., 1990; Moreno et al., 2005; Kostova et al., 2016). This reaction could explain the abundance of Ca-sulfate minerals (anhydrite and ettringite) in the studied FA and BA samples; however, slightly high Ca concentrations of FC samples could allow the reaction between CaO and aluminosilicate glass and Fe-oxides during combustion (Sokol et al., 2002; Vassilev et al., 2005b; Dai et al., 2014; Valentim et al., 2018). Thus, FeCa-rich glass and Ca-silicate minerals (e.g., gehlenite) in the crystalline phases were identified in the studied combustion residues (Figures 5a, 5b, 6a, 6b). In addition, lime, portlandite, and calcite were commonly identified in BA samples. Lime could easily convert to portlandite in the boiler during wet quenching in the boilers (Fernandez-Turiel et al., 2004); thus, portlandite is an abundant phase in the BA samples. Calcite in the BA samples is presumably primary calcite in the FCs due to the presence of partially reacted carbonates and unaffected coals in the studied BAs (Figures 5f and 5g).

4.2.3. Geochemistry

The average concentrations of the elements Ca, Mg, P, and Ti exceed 1000 µg/g in FA and BA (Table 4). Strontium is a major element in the FA samples and a minor one in the BA samples (Table 3). The elements Cr, Mn, Zn, Zr, Mo, and Ba are minor elements in both FA and BA samples; furthermore, the average As concentrations of studied FA samples also exceed 100 µg/g (Table 4). The average concentrations of elements Ca, Cu, As, Sr, Mo, and U in FA samples are generally higher than those of BA samples, while elements Li, Cr, Mn, Zn, Rb, Ba, W, and Pb display relatively higher concentrations in BA samples (Table 3). Magnesium, REYs, and the remaining trace elements display similar average concentrations in FA and BA (Table 4).

5. Discussion

5.1. Abundance and mode of occurrence of elements in feed coal

The average concentrations of the majority of minor and trace elements in the studied FC are mostly within the range of most world coals (Table 3). Nevertheless, in the comparison of average element concentrations with world low-rank coal averages, several elements are enriched in the studied FC samples (Ketris and Yudovich, 2009; Dai et al., 2016). Based on the enrichment classification by Dai et al. (2015a), the elements Mo (concentration coefficient (CC) = 45.9), Cs (CC = 20.0), and U (CC = 12.7) are significantly enriched, whereas the elements Zn, As, Sr, and Tl are enriched (10 > CC > 5). The slightly enriched elements (5 > CC > 2) in the studied FC samples are Li, P, Ti, Cr, Rb, Sb, Ta, and Pb. The average concentrations of the remaining elements are mostly close to the average values for low-rank coals (Table 4). Similar enrichment was also reported from mined coal seams and borehole samples in the Kangal coal deposit (Karayiğit et al., 2001b; Kalender and Karamazi, 2017).

The controlling factors of hazardous trace elements, as well as their occurrence in coals, are a widely studied topic. Therefore, several indirect (e.g., statistical analysis) and direct methods (e.g., SEM-EDX) were applied. The sole usage of the statistical methods could have some accuracy problems (Drew et al., 2008; Spears and Tewalt, 2009; Geboy et al., 2013). These problems could be overcome by applying direct methods such as SEM-EDX and selective leaching along with statistical methods (Eskenazy et al., 2010; Karayiğit et al., 2017a; Finkelman et al., 2018). Statistical analysis data show that ash yields display significant positive correlations with Ca (Table 5). As expected, this correlation and the high Ca contents are clearly related to the common presence of calcareous fossil shell remains and carbonate minerals in the studied FC samples. Calcium also shows significant positive correlations with Mn and Ba, and a moderate correlation with Sr (Table 5). The accessory presence of rhodochrosite in the FC samples could suggest a correlation between Ca and Mn. The element Sr is detected in some fossil shell remains by SEM-EDX. This could suggest that Sr is affiliated with carbonates in the studied samples; however, Ca, along with Sr, is commonly found in barites by SEM-EDX. Barite is generally the main carrier of Ba in coal, and the accessory presence of barite could explain its enrichment in the studied FC samples (Dai et al., 2006a; Zhao et al., 2014). Additionally, Ca and Ba were also detected in feldspars, and celsian is another source of Ba in the FC samples. Even though Ca and P do not display any correlation, Ca is traced in monazite by SEM-EDX and apatite is a minor phase in the FC samples. Therefore, Ca displays inorganic affinity in the studied FC samples. Traceable Ca, on the other hand, is also detected in organic matter of the samples.

Titanium is another major element displaying positive correlation with the ash yield, Mg, REY, and enriched trace elements (e.g., Li, Cs, Cr, Zn, Rb, and Pb) in the studied FC samples (Table 5). More interestingly, no significant correlation between Mg and ash yield was recorded, but Mg also displays similar positive correlations with several

Table 5. Elemental affinities with ash yields (%, dry) and each other deduced from the calculation of Pearson's correlation coefficients (correlation in table is significant at 0.01 level, 2-tailed; otherwise, an asterisk indicates that correlation is significant at 0.05 level, 2-tailed).

Correlation with ash content 0.60 < r < 1.0
Ca, Sc, Mn, Sr, Cs, Ba, Pb, Eu 0.40 < r < 0.6
Ti, Y*, Zr, Nb, La, Ce, Pr*, Nd*, Sm*, Gd*, Tb*, Dy*, Ho*, Er, Tm, Yb, Lu, Th
r ≥ –0.40
Total sulfur (–0.67), Tl (–0.51), U* (–0.41)
Correlation with Ti content 0.60 < r < 1.0
Mg, Sc, Cr, Cu, Zn, Ga, Rb, Sr, Cs, Nb, LREY, Eu, Gd, Yb, Th, W
0.40 < r < 0.6
Li, Be*, Mn*, As*, Y, Dy, Ho, Er, Tm, W, Pb*
Correlation with Ca content Mn (0.86), Ba (0.71), Sr* (0.43)
Correlation with total sulfur P (0.57), Tl (0.62), U* (0.48)

trace elements and REY (Table 4). In the FC samples, there are traces of the elements Mg and Ti in clay minerals examined under SEM-EDX. Cs enrichment is commonly reported from Turkish Neogene coals, and its enrichment is generally explained by the presence of detrital clay minerals in coals (Karayiğit et al., 2000, 2017a; Palmer et al., 2004). As expected, Cs displays positive correlations with ash yields, Mg, and Ti (Table 5); thus, its enrichment is related to the presence of clay minerals in the studied FC samples. Another enriched element, Cr, displays higher concentrations in the Turkish Neogene coals, and it has an accessory presence of chromite, which comes from clastic inputs from Cr-bearing ophiolitic rocks in the basement, controlling Cr enrichment in Turkish Neogene coals (Karayiğit et al., 2000; Palmer et al., 2004; Esenlik et al., 2006). The clastic inputs from Pınarbaşı ophiolites could bring chromites into the Kangal paleomire. In contrast, chromites were not detected in the FC samples. However, clastic inputs from ophiolitic rocks could be easily weathered and transformed into clay minerals in the paleomire, and Cr could be incorporated into clay minerals (Brownfield et al., 1995; Ruppert et al., 2005; Karayiğit et al., 2017b). This could also explain positive correlations among Cr, Mg, and Ti. Thus, Mg, Ti, trace elements, and REY are associated with clay minerals in the studied FC samples. Moreover, the SEM-EDX data also demonstrate that Ti, trace elements, and REY are affiliated with other minerals. For instance, ilmenite, sphene, and Ti-oxides in the studied samples could be another source for Ti and zircon for Zr. Although no correlation between REY, Ca, and P is recorded, the accessory presence of monazite and REY-bearing apatite in the studied samples implies that REYs are also affiliated with phosphates in the studied samples. All of these lines of evidence suggest that clastic inputs from basement and synchronous volcanic rocks are a source for Ti and Mg, along with enriched trace elements such as Li, Cs, Cr, and Rb.

Statistical analyses show that Zn and Pb might be affiliated with clay minerals in the studied FC samples (Table 4). Besides, the accessory presence of sphalerite and galena suggest that Zn and Pb are affiliated with sulfide minerals in the FC samples rather than with clay minerals. Furthermore, S is also traced in the organic matter. Even though additional analyses are needed, high total S content of the studied FC samples might be related to organic matter. Molybdenum, As, and Tl enrichments are generally present in the sulfide minerals in coal, and these elements can be substituted with each other in pyrite (Dai et al., 2006b, 2015b; Kolker, 2012; López-Antón et al., 2013). However, in the studied FC samples, none of these elements are traced from pyrite, sphalerite, and galena through SEM-EDX examination. The lack of these elements in the sulfide minerals could be related to their dissolution from sulfide mineral, or more simply, their concentrations could be below the detection limit of the SEM equipment (Kolker, 2012). Furthermore, Mo, As, and Tl, along with U, are redox-sensitive elements and can be enriched in anoxic paleomire conditions (Querol et al., 1996; Dai et al., 2008; Siavalas et al., 2009; Chen et al., 2018a). Arsenic, Mo, Tl, and U show positive correlations with each other, and total S displays a positive correlation with Tl and U. Hence, enrichment of Mo, Tl, and U is possibly related to anoxic conditions during peat accumulation in the Kangal paleomire. A similar assumption was also proposed for the Kalburçayırı coal seams (Karayiğit et al., 2000; Kalender and Karamazi, 2017). Uranium and Th are also traced in monazite by SEM-EDX; thus, U enrichment could be partially related to phosphate minerals in the FC samples

and synchronous tuff/volcanic input into the Kangal paleomire (Arbuzov et al., 2011).

5.2. Abundance of elements in fly ash and bottom ashes

The studied FA and BA samples, compared to most world and European coal ash averages, are enriched in Li, Cr, Zn, As, Rb, Sr, Mo, Cs, Tl, Pb, and U (Moreno et al., 2005; Ketris and Yudovich, 2009). The samples also display higher concentrations in Ca, Zn, As, Sr, Mo, Cs, Ba, Tl, Pb, and U than other Turkish FAs and BAs (Karayigit et al., 2001a, 2005, 2006; Vassilev et al., 2005a; Esenlik et al., 2006; Fotopoulou et al., 2010). In the BA samples, Rb and Sb also have higher concentrations than other Turkish BAs.

The elemental enrichment in FA samples and differences between FA and BA samples could be controlled by volatilization of elements and/or formation of new minerals during combustion (Meij, 1994; Querol et al., 1995; Llorens et al., 2001; Goodarzi et al., 2008; Meij and te Winkel, 2009). Several indices were proposed in order to determine the behavior of elements during coal combustion in boilers (e.g., Meij, 1994; Goodarzi and Hower, 2008; Dai et al., 2010). In this study, relative enrichment index (Re) and f/b indices were calculated according to Eqs. (1) and (2) below to quantify the partitioning among fly ash, and bottom ash.

$$RE = ([X]_a / [X]_c) \times (\text{ash yield of coal}/100) \quad (1)$$

$$\text{f/b index} = ([X]_{FA} / [X]_{BA}) \quad (2)$$

In Eq. (1), $[X]_a$ and $[X]_c$ are the contents of element X in the fly or bottom ash and in the feed coal, respectively. RE ≈ 1 indicates that elements do not become volatile during combustion. Elements with low volatility could be enriched in bottom ash, and their RE_{BA} is higher than 1, whereas volatile elements in the boiler could completely/partially condensate in ESP on the ash particles and the RE_{FA} would be higher than 1 (Meij, 1994; Goodarzi, 2006; Dai et al., 2010). In Eq. (2), $[X]_{FA}$ and $[X]_{BA}$ are the contents of element X in the fly ash and bottom ash, respectively. The volatile elements display high f/b values and could be condensed totally or partially in fly ash, while low volatile elements are enriched in bottom ash and display low f/b values (Meij, 1994; Dai et al., 2010).

The elements in the studied FA and BA samples can be divided into four groups according to their RE and f/b values. Group I elements (As, Sr, Mo, Cd, Tl, Bi, U, and total S) display high f/b values (>1.30) and their RE_{FA} values are slightly higher than the RE_{BA} values (Table 6), suggesting that the elements in Group I are depleted in the bottom ash due to their volatile character during combustion in the boiler (Goodarzi, 2006; Meij, 1994; Meij and te Winkel, 2009). Their high f/b values relate to their retention in the studied FA samples; nevertheless, these elements could be easily volatilized and partially emitted into the atmosphere (Llorens et al., 2001; Meij and te Winkel, 2009; Dai et al.,

Table 6. The mass balance calculations from the Kangal power plant (RE_{FA}: enrichment factor in fly ash; RE_{BA}: enrichment factor in bottom ash; f/b: fly ash/bottom ash ratio).

Element	RE_{FA}	RE_{BA}	f/b
Ca %	1.28	1.07	1.19
Mg %	1.28	1.27	1.01
TS %	0.54	0.24	2.24
Li	1.33	1.59	0.84
Be	1.26	1.48	0.85
P	1.40	1.22	1.14
Sc	1.37	1.49	0.92
Ti	1.34	1.46	0.92
Cr	1.29	1.37	0.94
Mn	1.32	1.38	0.96
Co	1.26	1.24	1.01
Cu	1.39	1.26	1.10
Zn	1.20	1.35	0.89
Ga	1.32	1.42	0.93
Ge	0.94	0.80	1.18
As	1.10	0.62	1.77
Rb	1.35	1.76	0.77
Sr	1.31	0.86	1.53
Y	1.28	1.27	1.01
Zr	1.35	1.31	1.03
Nb	1.34	1.60	0.84
Mo	1.19	0.59	2.03
Cd	1.05	0.75	1.40
Sb	1.14	0.84	1.35
Cs	1.32	1.48	0.89
Ba	1.92	2.32	0.83
La	1.31	1.44	0.91
Ce	1.31	1.39	0.94
Pr	1.30	1.39	0.94
Nd	1.30	1.37	0.95
Sm	1.31	1.33	0.98
Eu	1.36	1.47	0.93
Gd	1.29	1.33	0.97
Tb	1.28	1.29	0.99
Dy	1.28	1.29	0.99
Ho	1.28	1.27	1.01
Er	1.28	1.27	1.01
Tm	1.28	1.26	1.02
Yb	1.29	1.26	1.03
Lu	1.31	1.28	1.02
Hf	1.33	1.26	1.06
Ta	1.34	1.41	0.96
W	1.20	1.70	0.71
Tl	0.98	0.69	1.42
Pb	1.29	1.63	0.79
Bi	1.23	0.67	1.84
Th	1.30	1.34	0.97
U	1.22	0.74	1.65

2010). Group II elements (Ca, P, Cu, and Hf) have slightly higher RE_{FA} than $RE_{BA,}$ and their f/b values are higher than 1.0 (Table 6). Their slight enrichment in FA samples implies that these elements are partially volatilized in the boilers and retained in the studied FA samples. In Turkish FAs and BAs, Ca displays relatively higher concentrations in the BA due to the abundance of secondary lime, portlandite, and Ca-bearing sulfates (Karayigit et al., 2001a, 2005, 2006; Vassilev et al., 2005a; Esenlik et al., 2006). In contrast to Turkish FAs and BAs, Ca concentrations of the FA samples are higher than those of BA. The abundance of Ca-bearing sulfate and lime in the studied FA samples could cause this difference. Furthermore, CaO and Ca-sulfates in the FA have a tendency to retain As, Mo, Cd, Tl, and U (Hower et al., 2009; López-Antón et al., 2013; Silva et al., 2014; Zhang et al., 2016; Wang et al., 2018). Therefore, the Group I elements were enriched in the studied FA samples. As mentioned previously, the presence of FeCa-rich glass in the FA samples could also result in high concentrations of Ca. The newly formed Ca-silicate minerals (e.g., gehlenite) can be another source for Ca in the FA samples. The elements Cu, Hf, Tl, and U can also combine with newly formed Ca-silicate and other aluminosilicates in the studied FA samples (Querol et al., 1995; Silva et al., 2014; Gong et al., 2016; Chen et al., 2018b). In some FA samples, U is detected in monazites by SEM-EDX, like in the FC samples, which could also explain the high amount of U in the studied FA samples. Overall, the enrichment of Group I and II elements in the FA samples was mainly controlled by their retention in CaO, sulfate, and Ca-silicate minerals, and to a lesser extent by the presence of primary minerals in the FA samples.

The elements Mg, Ti, Be, Sc, Cr, Mn, Cu, Zr, Ta, Th, and REY are in Group III and their f/b values are 1.0 (Table 6). These elements generally have close RE_{FA} and RE_{BA} values, indicating that Group III is evenly distributed in FA and BA samples. Thus, the elements of Group III are less volatile during combustion in the boiler than those of Groups I and II. The elements of Group III are affiliated with clay minerals in the studied FC samples and could be liberated as a result of broken-down clay minerals during combustion. The liberated elements could be retained in glass and/or newly formed aluminosilicate minerals and Fe-oxides during combustion (Querol et al., 1995; Vassilev et al., 2003; Zhao et al., 2018). With the formation of amorphous aluminosilicate glass, aluminosilicates and Fe-oxides form during combustion in the studied boiler, so the elements of Group III could also be retained in the studied FA samples (Querol et al., 1995; Li et al., 2012; Dai et al., 2014; Hower et al., 2018). The presence of unaffected clay minerals and sulfides could also be a source for Group III elements in the BA samples. Consequently, average concentrations of Mg, Ti, and other elements of Group III are nearly equal in both combustion residues. In addition, the primary accessory Ti-oxides, namely sphene and ilmenite, are Ti sources in both combustion residues. The primary apatite and monazite in the FA and BA samples can also be a source for Th and HREY in the FA and BA samples (Chelgani and Hower, 2018). The Group IV elements (Li, Zn, Ga, Rb, Nb, Cs, Ba, Pb, and LREY) have f/b values less than 1.0 and their RE_{BA} values are higher than the RE_{FA} values (Table 6). The major elements in Group IV generally display low volatility during combustion and are retained in BA (Querol et al., 1995; Dai et al., 2010, 2014; Zhao et al., 2018). The presence of unburned coal particles, along with unaffected clay minerals, barite, and apatite, seems to elevate their concentrations in the studied BA samples. Zinc and Pb, however, display a volatile character and are mostly enriched in FA (Córdoba et al., 2012; Song et al., 2013; Zhao et al., 2018). Interestingly, these elements are enriched in the studied BA samples and could be related to the presence of unaffected Pb-bearing sphalerite in the studied BA samples (Figure 6h). The low combustion efficiency of the boiler during the sampling period might have resulted in the presence of unaffected pyrite and sphalerite and, in turn, Zn and Pb enrichment in the studied BA samples.

6. Conclusions

The FC samples are characterized by high ash yields and total sulfur contents. The mineralogical composition and SEM-EDX data show that carbonate minerals and pyrites authigenically precipitated within the paleomire, whereas clay minerals and associated minerals (e.g., feldspars, apatite, and Ti-oxides) with clay mineral aggregates have a detrital origin and/or syngenetic volcanic inputs. The significantly enriched elements in FCs are Mo, Cs, and U, while Li, P, Ti, Cr, Zn, As, Rb, Sr, Sb, Ta, Tl, and Pb are normally enriched in comparison to most of the world's coals. The statistical analysis and SEM-EDX data show that Ca, Ti, Mg, and enriched trace elements such Li, Cr, Zn, Cs, Sr, and Pb are inorganically affiliated, and only Tl and U probably have organic affinity in FC. Furthermore, formation of anoxic conditions in the Kangal paleomire presumably resulted in Mo and U enrichment in FC.

The mineralogical compositions of FA and BA are quite similar and show that newly formed minerals during combustion are common. Nevertheless, unaffected sulfides, clay minerals, and carbonates were also identified in BA by SEM-EDX. Like in the FC, Mo, Cs, and U are significantly higher in FA and BA samples. The enrichment of Mo and U in FA and BA are related to retention of CaO and Ca-sulfate. Unaffected clay minerals might cause Cs enrichment in BA, whereas its enrichment in FA can be attributed to its retention by glass. The elements in the FA and BA are distinguished into four groups according to

their volatility during combustion. The elements of Group I are the most volatile elements during combustion and condensation on FA particles, while the elements of Group IV are not volatile or less volatile during combustion, being transferred to BA. Nevertheless, Zn and Pb in the BA seem to be related to the presence of unaffected pyrite and sphalerites due to the low combustion efficiency of the boiler during the sampling period. Even though this study was based on a certain period of time and a certain unit in the power plant, the results show a robust trend. Nevertheless, in order to have a better understanding of elemental enrichment in FA, further studies based upon unburned carbon particles and other units of the Kangal power plant are recommended. Overall, enriched elements and minerals in FA and BA suggest that their disposal should be undertaken with caution.

Acknowledgments

This study was supported by TÜBİTAK under the YDABÇAG-100Y006 project entitled "The distributions of some HAPs elements in feed coals and combustion residues of Kangal power plants". Conceptualization, methodology, and investigation were performed by Aİ Karayiğit and RA Gayer. Aİ Karayiğit and RG Oskay interpreted the data and compiled the manuscript. Special thanks to Dr T Onacak and P Fisher for their assistance at different stages of laboratory studies, to Dr S Dai and Dr C Johnson for their constructive comments during manuscript preparation, and to the administrators and engineers of the Kangal power plant for their help and permission for sampling. Finally, the authors would like to thank the anonymous reviewers for their comments and suggestions.

References

Akar G, Sen S, Yilmaz H, Arslan V, Ipekoglu U (2013). Characterization of ash deposits from the boiler of Yenikoy coal-fired power plant, Turkey. International Journal of Coal Geology 105: 85-90. doi: 10.1016/j.coal.2012.12.001

American Society for Testing and Materials (2003). Standard Test Method for Gross Calorific Value of Coal and Coke. West Conshohocken, PA, USA: ASTM International. doi: 10.1520/D5865-13

American Society for Testing and Materials (2008). Standard Test Method for Sulfur in the Analysis Sample of Coal and Coke Using High-Temperature Tube Furnace Combustion. West Conshohocken, PA, USA: ASTM International. doi: 10.1520/D4239-18E01

American Society for Testing and Materials (2011). Standard Test Method for Ash in the Analysis Sample of Coal and Coke from Coal. West Conshohocken, PA, USA: ASTM International. doi: 10.1520/D3174-12R18

American Society for Testing and Materials (2017). Standard Test Method for Volatile Matter in the Analysis Sample of Coal and Coke. West Conshohocken, PA, USA: ASTM International. doi: 10.1520/D3175-18

Arbuzov SI, Volostnov AV, Rikhvanov LP, Mezhibor AM, Ilenok SS (2011). Geochemistry of radioactive elements (U, Th) in coal and peat of northern Asia (Siberia, Russian Far East, Kazakhstan, and Mongolia). International Journal of Coal Geology 86: 318-328. doi: 10.1016/j.coal.2011.03.005

Baba A, Kaya A, Birsoy YK (2003). The effect of Yatagan thermal power plant (Mugla, Turkey) on the quality of surface and ground waters. Water Air Soil and Pollution 149: 93-111. doi: 10.1023/A:1025660629875

Basarir H, Karpuz C (2004). A rippability classification system for marls in lignite mines. Engineering Geology 74: 303-318. doi:10.1016/j.enggeo.2004.04.004

Bayat O (1998). Characterisation of Turkish fly ashes. Fuel 77: 1059-1066. doi: 10.1016/S0016-2361(97)00274-3

Bohor BF, Triplehorn DM (1993). Tonstein: Altered Volcanic Ash Layers in Coal-Bearing Sequences. Geological Society of America Special Paper 285. Boulder, CO, USA: Geological Society of America. doi: 10.1130/SPE285-p1

Brownfield ME, Affolter RH, Stricker GD, Hildebrand RT (1995). High chromium contents in Tertiary coal deposits of northwestern Washington-a key to their depositional history. International Journal of Coal Geology 27: 153-169. doi: 10.1016/0166-5162(94)00026-V

Bryant G, Bailey C, Wu H, McLennan A, Stanmore B et al. (1999). The significance of the high temperature behaviour of siderite grains during combustion. In: Gupta RP, Wall TF, Baxter L (editors). Impact of Mineral Impurities in Solid Fuel Combustion. New York, NY, USA: Kluwer Academic/Plenum Publications, pp. 581-594. doi: 10.1007/0-306-46920-0_43

Burger K, Bandelow FK, Bieg G (2000). Pyroclastic kaolin coal–tonsteins of the Upper Carboniferous of Zonguldak and Amasra, Turkey. International Journal of Coal Geology 45: 39-53. doi: 10.1016/S0166-5162(00)00021-5

Chelgani SC, Hower JC (2018). Estimating REY content of eastern Kentucky coal samples based on their associated ash elements. Journal of Rare Earths 36: 1234-1238. doi: 10.1016/j.jre.2018.02.015

Chen G, Sun Y, Yan B, Yang R, Liu B et al. (2018b). Distribution of trace elements during coal gasification: the effect of upgrading method. Journal of Cleaner Production 190: 193-199. doi: 10.1016/j.jclepro.2018.04.077

Chen J, Chen, P, Yao D, Huang W, Tang S et al. (2018a). Geochemistry of uranium in Chinese coals and the emission inventory of coal-fired power plants in China. International Geological Review 60: 621-637. doi: 10.1080/00206814.2017.1295284

Córdoba P, Ochoa-Gonzalez R, Font O, Izquierdo M, Querol X et al. (2012). Partitioning of trace inorganic elements in a coal-fired power plant equipped with a wet flue gas desulphurisation system. Fuel 92: 145-157. doi: 10.1016/j.fuel.2011.07.025

Creelman RA, Ward CR, Schumacher G, Juniper L (2013). Relation between coal mineral matter and deposit mineralogy in pulverized fuel furnaces. Energy and Fuels 27: 5714-5724. doi: 10.1021/ef400636q

Dai S, Han D, Chou CL (2006a). Petrography and geochemistry of the Middle Devonian coal from Luquan, Yunnan Province, China. Fuel 85: 456-464. doi: 10.1016/j.fuel.2005.08.017

Dai S, Li T, Jiang Y, Ward CR, Hower JC et al. (2015b). Mineralogical and geochemical compositions of the Pennsylvanian coal in the Hailiushu Mine, Daqingshan Coalfield, Inner Mongolia, China: implications of sediment-source region and acid hydrothermal solutions. International Journal of Coal Geology 137: 92-110. doi: 10.1016/j.coal.2014.11.010

Dai S, Liu J, Ward CR, Hower JC, French D et al. (2016). Mineralogical and geochemical compositions of Late Permian coals and host rocks from the Guxu Coalfield, Sichuan Province, China, with emphasis on enrichment of rare metals. International Journal of Coal Geology 166: 71-95. doi: 10.1016/j.coal.2015.12.004

Dai S, Ren D, Zhou Y, Chou CL, Wang X et al. (2008). Mineralogy and geochemistry of a superhigh-organic-sulfur coal, Yanshan Coalfield, Yunnan, China: evidence for a volcanic ash component and influence by submarine exhalation. Chemical Geology 255: 182-194. doi: 10.1016/j.chemgeo.2008.06.030

Dai S, Seredin VV, Ward CR, Hower JC, Xing Y et al. (2015a). Enrichment of U–Se–Mo–Re–V in coals preserved within marine carbonate successions: geochemical and mineralogical data from the Late Permian Guiding Coalfield, Guizhou, China. Mineralium Deposita 50: 159-186. doi: 10.1007/s00126-014-0528-1

Dai S, Ward CR, Graham IT, French D, Hower JC et al. (2017). Altered volcanic ashes in coal and coal-bearing sequences: a review of their nature and significance. Earth-Science Reviews 175: 44-74. doi: 10.1016/j.earscirev.2017.10.005

Dai S, Zeng R, Sun Y (2006b). Enrichment of arsenic, antimony, mercury, and thallium in a Late Permian anthracite from Xingren, Guizhou, Southwest China. International Journal of Coal Geology 66: 217-226. doi: 10.1016/j.coal.2005.09.001

Dai S, Zhao L, Hower JC, Johnston MN, Song W et al. (2014). Petrology, mineralogy, and chemistry of size-fractioned fly ash from the Jungar power plant, Inner Mongolia, China, with emphasis on the distribution of rare earth elements. Energy and Fuels 28: 1502-1514. doi: 10.1021/ef402184t

Dai S, Zhao L, Peng S, Chou CL, Wang X et al. (2010). Abundances and distribution of minerals and elements in high-alumina coal fly ash from the Jungar Power Plant, Inner Mongolia, China. International Journal of Coal Geology 81: 320-332. doi: 10.1016/j.coal.2009.03.005

Drew LJ, Grunsky EC, Schuenemeyer JH (2008). Investigation of the structure of geological process through multivariate statistical analysis-the creation of a coal. Mathematical Geosciences 40: 789-811. doi: 10.1007/s11004-008-9176-2

Erol M, Genç A, Öveçoğlu ML, Yücelen E, Küçükbayrak S et al. (2000). Characterization of a glass-ceramic produced from thermal power plant fly ashes. Journal of European Ceramic Society 20: 2209-2214. doi: 10.1016/S0955-2219(00)00099-6

Esenlik S, Karayigit AI, Bulut Y, Querol X, Alastuey A et al. (2006). Element behaviour during combustion in coal-fired Orhaneli power plant, Bursa-Turkey. Geologica Acta 4: 439-449. doi: 10.1344/105.000000345

Eskenazy GM, Finkelman RB, Chattarjee S (2010). Some considerations concerning the use of correlation coefficients and cluster analysis in interpreting coal geochemistry data. International Journal of Coal Geology 83: 491-493. doi: 10.1016/j.coal.2010.05.006

Fernandez-Turiel JL, Georgakopoulos A, Gimeno D, Papastergios G, Kolovos N (2004). Ash deposition in a pulverized coal-fired power plant after high-calcium lignite combustion. Energy and Fuels 18: 1512-1518. doi: 10.1021/ef0400161

Filippidis A, Georgakopoulos A, Kassoli-Fournaraki A (1996). Mineralogical components of some thermally decomposed lignite and lignite ash from the Ptolemais basin, Greece. International Journal of Coal Geology 30: 303-314. doi: 10.1016/0166-5162(95)00049-6

Finkelman RB, Palmer CA, Wang P (2018). Quantification of the modes of occurrence of 42 elements in coal. International Journal of Coal Geology 185: 138-160. doi: 10.1016/j.coal.2017.09.005

Fotopoulou M, Siavalas G, İnaner H, Katsanou K, Lambrakis N et al. (2010). Combustion and leaching behavior of trace elements in lignite and combustion by-products from the Muğla basin, SW Turkey. Bulletin of the Geological Society of Greece 43: 2218-2228.

Gayer RA, Rose M, Dehmer J, Shao LY (1999). Impact of sulphur and trace element geochemistry on the utilization of a marine-influenced coal-case study from the South Wales Variscan foreland basin. International Journal of Coal Geology 40: 151-174. doi: 10.1016/S0166-5162(98)00066-4

Geboy NJ, Engle MA, Hower JC (2013). Whole-coal versus ash basis in coal geochemistry: a mathematical approach to consistent interpretations. International Journal of Coal Geology 113: 41-49. doi: 10.1016/j.coal.2013.02.008

Gong B, Tian C, Xiong Z, Zhao Y, Zhang J (2016). Mineral changes and trace element releases during extraction of alumina from high aluminum fly ash in Inner Mongolia, China. International Journal of Coal Geology 166: 96-107. doi: 10.1016/j.coal.2016.07.001

Goodarzi F (2006). Assessment of elemental content of milled coal, combustion residues, and stack emitted materials: possible environmental effects for a Canadian pulverized coal-fired power plant. International Journal of Coal Geology 65: 17-25. doi: 10.1016/j.coal.2005.04.006

Goodarzi F, Hower JC (2008). Classification of carbon in Canadian fly ashes and their implications in the capture of mercury. Fuel 87, 1949-1957. doi: 10.1016/j.fuel.2007.11.018

Goodarzi F, Huggins F, Sanei H (2008). Assessment of elements, speciation of As, Cr, Ni and emitted Hg for a Canadian power plant burning bituminous coal. International Journal of Coal Geology 74: 1-12. doi: 10.1016/j.coal.2007.09.002

Hower JC, Groppo JG, Graham UM, Ward CR, Kostova IJ et al. (2017). Coal-derived unburned carbons in fly ash: a review. International Journal of Coal Geology 179: 11-27. doi: 10.1016/j.coal.2017.05.007

Hower JC, Qian D, Briot NJ, Henke KR, Hood MM et al. (2018). Rare earth element associations in the Kentucky State University stoker ash. International Journal of Coal Geology 189: 75-82. doi: 10.1016/j.coal.2018.02.022

Hower JC, Robl TL, Thomas G, Hopps SD, Grider M (2009). Chemistry of coal and coal combustion products from Kentucky power plants: results from the 2007 sampling, with emphasis on selenium. Coal Combustion and Gasification Products 1: 50-62. doi: 10.4177/CCGP-D-09-0013.1

Huffman GP, Huggins FE, Levasseur AA, Chow O, Srinivasachar S et al. (1989). Investigation of the transformations of pyrite in a drop-tube furnace. Fuel 68: 485-490. doi: 10.1016/0016-2361(89)90271-8

Huffman GP, Huggins FE, Shah N, Shah A (1990). Behavior of basic elements during coal combustion. Progress in Energy and Combustion Science 16: 243-251. doi: 10.1016/0360-1285(90)90033-Y

Kalender L, Karamazı K (2017). A comparison of the Kalburçayırı lignites in the Kangal-Sivas basin and various worldwide coal compositions. International Journal of Oil, Gas and Coal Technology 15: 394-410. doi: 10.1504/IJOGCT.2017.10003100

Karayiğit Aİ, Bircan C, Mastalerz M, Oskay RG, Querol X et al. (2017b). Coal characteristics, elemental composition and modes of occurrence of some elements in the İsaalan coal (Balıkesir, NW Turkey). International Journal of Coal Geology 172: 43-59. doi: 10.1016/j.coal.2017.01.016

Karayigit AI, Bulut Y, Karayigit G, Querol X, Alastuey A et al. (2006). Mass balance of major and trace elements in a coal-fired power plant. Energy Sources Recovery, Utilization, and Environmental Effects 28: 1311-1320. doi: 10.1080/009083190910523

Karayigit AI, Bulut Y, Querol X, Alastuey A, Vassilev S (2005). Variations in fly ash composition from the soma power plant, Turkey. Energy Sources 27: 1473-1481. doi: 10.1080/009083190523811

Karayigit AI, Gayer RA, Ortac FE, Goldsmith S (2001b). Trace elements in the Lower Pliocene fossiliferous Kangal lignites, Sivas, Turkey. International Journal of Coal Geology 47: 73-89. doi: 10.1016/S0166-5162(01)00030-1

Karayigit AI, Gayer RA, Querol X, Onacak T (2000). Contents of major and trace elements in feed coals from Turkish coal-fired power plants. International Journal of Coal Geology 44: 169-184. doi: 10.1016/S0166-5162(00)00009-4

Karayiğit Aİ, Littke R, Querol X, Jones T, Oskay RG et al. (2017a). The Miocene coal seams in the Soma Basin (W. Turkey): insights from coal petrography, mineralogy and geochemistry. International Journal of Coal Geology 173: 110-128. doi: 10.1016/j.coal.2017.03.004

Karayiğit Aİ, Mastalerz M, Oskay RG, Gayer RA (2018). Coal petrography, mineralogy, elemental compositions and palaeoenvironmental interpretation of Late Carboniferous coal seams in three wells from the Kozlu coalfield (Zonguldak Basin, NW Turkey). International Journal of Coal Geology 187: 54-70. doi: 10.1016/j.coal.2017.12.007

Karayigit AI, Onacak T, Gayer RA, Goldsmith S (2001a). Mineralogy and geochemistry of feed coals and their combustion residues from the Cayirhan power plant, Ankara, Turkey. Applied Geochemistry 16: 911-919. doi: 10.1016/S0883-2927(00)00061-5

Ketris MP, Yudovich YE (2009). Estimations of Clarkes for carbonaceous biolithes: world averages for trace element contents in black shales and coals. International Journal of Coal Geology 78: 135-148. doi: 10.1016/j.coal.2009.01.002

Koçaslan A, Yüksek AG, Görgülü K, Arpaz E (2017). Evaluation of blast-induced ground vibrations in open-pit mines by using adaptive neuro-fuzzy inference systems. Environmental Earth Sciences 76: 57. doi: 10.1007/s12665-016-6306-x

Kolker A (2012). Minor element distribution in iron disulfides in coal: a geochemical review. International Journal of Coal Geology 94: 32-43. doi: 10.1016/j.coal.2011.10.011

Kostova I, Vassileva C, Dai S, Hower JC (2016). Mineralogy, geochemistry and mercury content characterization of fly ashes from the Maritza 3 and Varna thermoelectric power plants, Bulgaria. Fuel 186: 674-684. doi: 10.1016/j.fuel.2016.09.015

Koukouzas N, Ward CR, Li Z (2010). Mineralogy of lignites and associated strata in the Mavropigi field of the Ptolemais Basin, northern Greece. International Journal of Coal Geology 81: 182-190. doi: 10.1016/j.coal.2009.12.012

Kuşcu İ, Tosdal RM, Gencalioğlu-Kuşcu G, Friedman R, Ullrich TD (2013). Late Cretaceous to Middle Eocene magmatism and metallogeny of a portion of the southeastern Anatolian orogenic belt, east-central Turkey. Economic Geology 106: 641-666. doi: 10.2113/econgeo.108.4.641

Li J, Zhuang X, Querol X, Font O, Moreno N et al. (2012). Environmental geochemistry of the feed coals and their combustion by-products from two coal-fired power plants in Xinjiang province, Northwest China. Fuel 95: 446-456. doi: 10.1016/j.fuel.2011.10.025

Llorens JF, Fernández-Turiel JL, Querol X (2001). The fate of trace elements in a large coal-fired power plant. Environmental Geology 40: 409-416. doi: 10.1007/s002540000191

López-Antón AM, Spears DA, Somoano MD, Martínez Tarazona MR (2013). Thallium in coal: analysis and environmental implications. Fuel 105: 13-18. doi: 10.1016/j.fuel.2012.08.004

Marschik R, Spikings R, Kuşcu I (2008). Geochronology and stable isotope signature of alteration related to hydrothermal magnetite ores in Central Anatolia, Turkey. Mineralium Deposita 43:111-124. doi: 10.1007/s00126-007-0160-4

McLennan AR, Bryant GW, Bailey CW, Stanmore BR, Wall TF (2000). An experimental comparison of the ash formed from coals containing pyrite and siderite mineral in oxidizing and reducing conditions. Energy and Fuels 14: 308-315. doi: 10.1021/ef990092h

Meij R (1994). Trace element behavior in coal-fired power plants. Fuel Processing Technology 39: 199-217. doi: 10.1016/0378-3820(94)90180-5

Meij R, te Winkel BH (2009). Trace elements in world steam coal and their behaviour in Dutch coal-fired power stations: a review. International Journal of Coal Geology 77: 289-293. doi: 10.1016/j.coal.2008.07.015

Moreno N, Querol X, Andrés JM, Stanton K, Towler M et al. (2005). Physico-chemical characteristics of European pulverized coal combustion fly ashes. Fuel 84: 1351-1363. doi: 10.1016/j.fuel.2004.06.038

Narin R, Kavuşan G (1993). Geology of the Kalburçayırı lignite basin, Sivas-Kangal Turkey. Bulletin of the Faculty of Engineering, Cumhuriyet University, Series A, Earth Science 10: 43-47.

Oskay RG, Christanis K, Inaner H, Salman M, Taka M (2016). Palaeoenvironmental reconstruction of the eastern part of the Karapınar-Ayrancı coal deposit (Central Turkey). International Journal of Coal Geology 163: 100-111. doi: 10.1016/j.coal.2016.06.022

Oskay RG, Inaner H, Karayiğit Aİ, Christanis K (2013). Coal deposits of Turkey: properties and importance on energy demand. Bulletin of the Geological Society of Greece 47: 2111-2120.

Palmer CA, Tuncali E, Dennen KO, Coburn TC, Finkelman RB (2004). Characterization of Turkish coals: a nationwide perspective. International Journal of Coal Geology 60, 85-115. doi: 10.1016/j.coal.2004.05.001

Querol X, Cabrera L, Pickel W, López-Soler A, Hagemann HW et al. (1996). Geological controls on the coal quality of the Mequinenza subbituminous coal deposit, northeast Spain. International Journal of Coal Geology 29: 67-91. doi: 10.1016/0166-5162(95)00009-7

Querol X, Fernandez-Turiel JL, López-Soler A (1994). The behaviour of mineral matter during combustion of Spanish subbituminous and brown coals. Mineralogical Magazine 58: 119-133. doi: 10.1180/minmag.1994.058.390.11

Querol X, Fernandez-Turiel JL, López-Soler A (1995). Trace elements in coal and their behaviour during combustion in a large power station. Fuel 74: 331-343. doi: 10.1016/0016-2361(95)93464-O

Querol X, Whateley MKG, Fernández-Turiel JL, Tuncali E (1997). Geological controls on the mineralogy and geochemistry of the Beypazari lignite, central Anatolia, Turkey. International Journal of Coal Geology 33: 255-271. doi: 10.1016/S0166-5162(96)00044-4

Reifenstein AP, Kahraman H, Coin CDA, Calos NJ, Miller G et al. (1999). Behaviour of selected minerals in an improved ash fusion test: quartz, potassium feldspar, sodium feldspar, kaolinite, illite, calcite, dolomite, siderite, pyrite and apatite. Fuel 78: 1449-1461. doi: 10.1016/S0016-2361(99)00065-4

Rudmin M, Ruban A, Savichev O, Mazurov A, Dauletova A et al. (2018). Authigenic and detrital minerals in peat environment of Vasyugan swamp, Western Siberia. Minerals 8: 500. doi: 10.3390/min8110500

Ruppert LF, Hower JC, Eble CF (2005). Arsenic-bearing pyrite and marcasite in the Fire Clay coal bed, Middle Pennsylvanian Breathitt Formation, eastern Kentucky. International Journal of Coal Geology 63: 27-35. doi: 10.1016/j.coal.2005.02.003

Siavalas G, Linou M, Chatziapostolou A, Kalaitzidis S, Papaefthymiou H et al. (2009). Palaeoenvironment of Seam I in the Marathousa Lignite Mine, Megalopolis Basin (Southern Greece). International Journal of Coal Geology 78: 233-248. doi: 10.1016/j.coal.2009.03.003

Silva LFO, Oliveira MLS, Kautzmann RM, Ramos CG, Izquierdo M et al. (2014). Geochemistry and mineralogy of coal-fired circulating fluidized bed combustion fly ashes. Coal Combustion and Gasification Products 6: 16-28. doi: 10.4177/CCPG-D-14-00005.1

Sokol EV, Kalugin VM, Nigmatulina EN, Volkova NI, Frenkel AE et al. (2002). Ferrospheres from fly ashes of Chelyabinsk coals: chemical composition, morphology and formation conditions. Fuel 81: 867-876. doi: 10.1016/S0016-2361(02)00005-4

Song W, Jiao F, Yamada N, Ninomiya Y, Zhu Z (2013). Condensation behavior of heavy metals during oxy-fuel combustion: deposition, species distribution, and their particle characteristics. Energy and Fuels 27: 5640-5652. doi: 10.1021/ef400484p

Spears DA, Tewalt SJ (2009). The geochemistry of environmentally important trace elements in UK coals, with special reference to the Parkgate coal in the Yorkshire-Nottinghamshire Coalfield, UK. International Journal of Coal Geology 80: 157-166. doi: 10.1016/j.coal.2009.08.010

Spliethoff H, Greul U, Rüdiger H, Hein KRG (1996). Basic effects on NOx emissions in air staging and reburning at a bench-scale test facility. Fuel 75: 560-564. doi: 10.1016/0016-2361(95)00281-2

Styszko-Grochowiak K, Gołłaś J, Jankowski H, Koziński S (2004). Characterization of the coal fly ash for the purpose of improvement of industrial on-line measurement of unburned carbon content. Fuel 83: 1847-1853. doi: 10.1016/j.fuel.2004.03.005

Suárez-Ruiz I, Valentim B, Borrego AG, Bouzinos A, Flores D et al. (2017). Development of a petrographic classification of fly-ash components from coal combustion and co-combustion (an ICCP classification system, Fly-Ash Working Group – Commission III). International Journal of Coal Geology 183: 188-203. doi: 10.1016/j.coal.2017.06.004

Swaine DJ (1990). Trace Elements in Coal. London, UK: Butterworths.

Tercan AE, Karayigit AI (2001). Estimation of lignite reserve in the Kalburcayiri field, Kangal basin, Sivas, Turkey. International Journal of Coal Geology 47: 91-100. doi: /10.1016/S0166-5162(01)00033-7

Toprak S, Yalcin Erik N (2011). Petrographical properties and unusual features of Kangal coals, Sivas-Turkey. International Journal of Coal Geology 86: 297-305. doi: 10.1016/j.coal.2011.03.002

Tuncalı E, Çiftci B, Yavuz N, Toprak S, Köker A et al. (2002). Chemical and Technological Properties of Turkish Tertiary Coals. Ankara, Turkey: MTA Publication.

Turhan S, Gören E, Garad AMK, Altıkulaç A, Kurnaz A et al. (2018). Radiometric measurement of lignite coal and its by-products and assessment of the usability of fly ash as raw materials in Turkey. Radiochimica Acta 106: 611-621. doi: 10.1515/ract-2017-2863

Valentim B, Białecka B, Gonçalves PA, Guedes A, Guimarães R et al. (2018). Undifferentiated inorganics in coal fly ash and bottom ash: calcispheres, magnesiacalcispheres, and magnesiaspheres. Minerals 8: 140. doi: 10.3390/min8040140

Valentim B, Shreya N, Paul B, Gomes CS, Sant'Ovaia H et al. (2016). Characteristics of ferrospheres in fly ashes derived from Bokaro and Jharia (Jharkand, India) coals. International Journal of Coal Geology 153: 52-74. doi: 10.1016/j.coal.2015.11.013

Vassilev SV, Menendez R, Alvarez D, Diaz-Somoano M, Martínez-Tarazona MR (2003). Phase-mineral and chemical composition of coal fly ashes as a basis for their multicomponent utilization. 1. Characterization of feed coals and fly ashes. Fuel 82: 1793-1811. doi: 10.1016/S0016-2361(03)00123-6

Vassilev SV, Vassileva CG (1996). Mineralogy of combustion wastes from coal-fired power stations. Fuel Processing Technology 47: 261-280. doi: 10.1016/0378-3820(96)01016-8

Vassilev SV, Vassileva CG, Karayigit AI, Bulut Y, Alastuey A et al. (2005a). Phase-mineral and chemical composition of composite samples from feed coals, bottom ashes and fly ashes at the Soma power station, Turkey. International Journal of Coal Geology 61: 35-63. doi: 10.1016/j.coal.2004.06.004

Vassilev SV, Vassileva CG, Karayigit AI, Bulut Y, Alastuey A et al. (2005b). Phase-mineral and chemical composition of fractions separated from composite fly ashes at the Soma power station, Turkey. International Journal of Coal Geology 61: 65-85. doi: 0.1016/j.coal.2004.05.004

Wang C, Liu H, Zhang Y, Zou C, Anthony EJ (2018). Review of arsenic behavior during coal combustion: volatilization, transformation, emission and removal technologies. Progress in Energy and Combustion Science 68: 1-28. doi: 0.1016/j.pecs.2018.04.001

Ward CR (2016). Analysis, origin and significance of mineral matter in coal: an updated review. International Journal of Coal Geology 165: 1-27. doi: 10.1016/j.coal.2016.07.014

Ward CR, French D (2006). Determination of glass content and estimation of glass composition in fly ash using quantitative X-ray diffractometry. Fuel 85: 2268-2277. doi: 10.1016/j.fuel.2005.12.026

Yalçin Erik N (2011). Hydrocarbon generation potential and Miocene-Pliocene paleoenvironments of the Kangal Basin (Central Anatolia, Turkey). Journal of Asian Earth Sciences 42: 1146-1162. doi: 10.1016/j.jseaes.2011.06.013

Yağmurlu F, Toker E, Şentürk M (2016). The coal-quality distribution of lignite deposits and tectono-sedimentary evolution of Etyemez in Kangal Neogene basin (Central Anatolia, Turkey). International Journal of Oil, Gas and Coal Technology 11: 75-92. doi: 10.1504/IJOGCT.2016.073781

Yilmaz G (2012). Structural characterization of glass-ceramics made from fly ash containing SiO2-Al2O3-Fe2O3-CaO and analysis by FT-IR-XRD-SEM methods. Journal of Molecular Structure 1019: 37-42. doi: 10.1016/j.molstruc.2012.03.028

Zhang Y, Shi M, Wang J, Yao J, Cao Y et al. (2016). Occurrence of uranium in Chinese coals and its emissions from coal-fired power plants. Fuel 166: 404-409. doi: 10.1016/j.fuel.2015.11.014

Zhao CL, Sun YZ, Xiao L, Qin SJ, Wang JX et al. (2014). The occurrence of barium in a Jurassic coal in the Huangling 2 Mine, Ordos Basin, northern China. Fuel 128: 428-432. doi: 10.1016/j.fuel.2014.03.040

Zhao S, Duan Y, Li Y, Liu M, Lu J et al. (2018). Emission characteristic and transformation mechanism of hazardous trace elements in a coal-fired power plant. Fuel 214: 597-606. doi: 10.1016/j.fuel.2017.09.093